A Temperature Compensated Smart Nitrate-Sensor for Agricultural Industry

Md. Eshrat E Alahi, *Student Member, IEEE*, Xie Li, *Subhas Mukhopadhyay*, *Fellow Member, IEEE, Lucy Burkitt*

***Abstract*— Extended research on the design and development of a smart nitrate sensor for monitoring nitrate concentration in surface and groundwater, are reported in this paper. The developed portable sensing system consists of a planar interdigital sensor, associated electronics, instrumentation and Electrochemical Impedance Spectroscopy (EIS) based analysis. The system is capable of measuring nitrate concentrations in the range of 0.01 to 0.5 mg/L in ground and surface water. This study extends our earlier work by including a temperature compensation capacity within the sensor. WiFi-based Internet of Things (IoT) has been included making it a connected sensing system. The system is capable of sending data directly to an IoT-based web server, which will be useful to develop distributed monitoring systems in the future. The developed system has the potential to monitor the impact of industrial, agricultural or urban activity on water quality, in real-time.**

***Index Terms*— Agricultural industry, Electrochemical impedance spectroscopy, Interdigital sensor, IoT-enabled sensor node, Nitrate detection, Water quality.**

INTRODUCTION

In an agricultural country like New Zealand, the concentration of nitrate in surface and groundwater is concerning and has been identified as a critical issue facing New Zealand's future [1]. Dairy farming, disposal of human and animal sewage, urban runoff and industrial waste to land or into waterways have been identified as sources of nitrate [2]. Nitrate-nitrogen (NO_3–N) is a fundamental element for the growth of all plants and animals, as it is a major component of the supply of protein. It is used in the agricultural sector to increase plant and livestock production. However, nitrate can become an issue if its concentration in surface water rises above a certain threshold, and this issue is commonly associated with agricultural areas [3, 4]. In New Zealand, cattle urination from dairy farming is the largest source of nitrate contamination [5] as the highly concentrated nitrate deposits leach into groundwater, which ultimately increases the nitrate concentration of surface water. Elevated nitrate-N concentrations in surface waters can stimulate the growth of unwanted algae and aquatic plants [6]. High nitrate-N concentrations change the pH of the water and lower oxygen concentrations, affecting aquatic life and degrading fish habitats [7]. Elevated nitrate concentrations in drinking water, can also lead to blue baby syndrome [8]. According to Environment Protection Agency (EPA), the acceptable level of nitrate-N in drinking water is 10 mg/L [9].

The spectrophotometric method is commonly used to detect nitrate-nitrogen (NO_3-N) in water using specific chemical reagents [10, 11]. In other research, vanadium has been utilized for the reduction of nitrate ions by acidic Griess reaction [12]. Other detection methods include ion chromatography [13], palladium nanostructures [14], planar electrode sensors [15], ion selective electrodes [16], and optical fiber sensors [17, 18]. In situ detection of nitrate in soil moisture using impedance spectroscopy, have also been reported [19, 20].

The regional councils around New Zealand monitor water samples from rivers, lakes and groundwater in a routine manner. The samples are collected by staff at a regular interval of time, usually on a monthly basis [21]. The concentrations of nitrate-N is measured by spectrophotometric method. Typically, nitrate-N concentrations change with increasing and decreasing stream or river flows. Therefore, a monthly sampling regime may not adequately represent the actual nitrate-N profile. This could influence the understanding of the seasonal effects on nitrate-N loss as well as total loads of nitrate-N estimated to be leaving a catchment. This information is critical for regional councils to implement policy and management accurately. Although high-frequency nitrate sensors are commercially available, these sensors cost in the order of $7,500-35,000 USD and are designed to measure nitrate concentrations of > 1 mg/L, which is often not sensitive enough for New Zealand waterways. Therefore, there is a clear need for low-cost, low concentration, real-time, smart nitrate sensors and sensing systems, to measure nitrate concentrations in water.

The objective of this research is to extend our earlier work to develop a low-cost, in-situ real-time monitoring system based on the planar interdigital sensor. The purpose is to achieve continuous assessment of nitrate-N in water to

Manuscript received December 09, 2016; revised February 27, 2017; accepted April 06, 2017.

Md. Eshrat E Alahi and Subhas Mukhopadhyay are with the Department of Engineering, Macquarie University, Sydney, NSW 2109, Australia (e-mail: ealahi@yahoo.com).

Xie Li was and Lucy Burkitt is with Massey University, Palmerston North 4474, New Zealand.

improve our understanding and measurement of seasonal and annual losses of nitrate to waterways [21, 22]. The earlier work as reported in [21] provides experimental results of the prototype sensor, which are obtained under laboratory environmental condition. The earlier reported system provided good accuracy under a controlled environment. However, the ambient temperature under field conditions vary considerably. Therefore, the performance of the developed system suffered due to temperature fluctuations. Therefore, a compensation of the effect of temperature was required in the current system. The system can transfer measured data to a cloud server for further analysis, saving staff time in collecting samples. The availability of Internet of Things (IoT) allows the system to be developed as part of a distributed network. The main contributions of this paper are 1. the use of a temperature compensated interdigital capacitive sensor to measure nitrate at low concentrations and 2. the development of a low-cost (the estimated amount of the whole system's cost is less than $100 USD) sensing system for continuous nitrate measurement which links to an IoT-based cloud server through an integrated WiFi connection. The experimental development, evaluation and validation of the systems performance are explained.

SENSOR AND EXPERIMENTAL SETUP

A. Operating Principle of the Interdigital Sensor

Planar type interdigital sensors [23, 24] have been used for the detection of nitrate-N in water samples for this research. Planar interdigital sensors behave like parallel plate capacitors and the principle of detection is based on a change of electric field generated between two types of electrodes. A low amplitude alternating electrical voltage is applied across the sensor terminals. The generated electric field passes through material under test (MUT) so that the electric field will be affected. The magnitude and phase of the impedance of the sensor is measured. The real and imaginary components of the impedance are used to determine the properties of the material under test. For measurement of nitrate contamination in water, a thin-film layer Parylene coated interdigital sensor has been used. Fig. 1 shows the fabricated sensor, one out of 36 sensors in a 4-inch wafer. Since the sensor is exposed to air

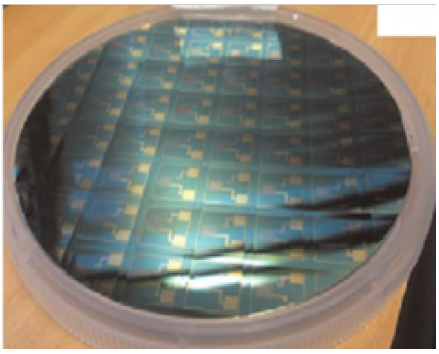

Fig. 1. Fabricated wafer of thin film electrode sensor

and dipped in water, the potential for oxidation is a real problem. Parylene coating on the sensing surface protects the sensor from oxidation due to moisture and Faradic currents. Different types of sensors have been fabricated and the current research is based on 1-5-50. The 1-5-50 configuration means a repeated pattern of five sensing electrodes (-ve electrode) for one excitation electrode (+ve electrode), with a distance of 50 μm between two consecutive electrodes [25]. The sensing area was fixed to 2.5 mm X 2.5 mm. Fig. 2 shows the Parylene

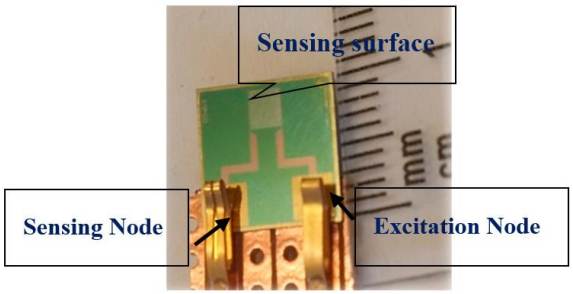

Fig. 2. Interdigital sensor with Parylene coating

coated sensor, which has been used in all experiments.

B. Experimental Setup

Temperature affects the mobility of ions in water [26], therefore, it is important to measure the changing behavior of the sensor at different temperatures. Fig. 3 shows the experimental setup involving a high precision Hioki 3522-50 LCR meter, Hioki 4-terminal probe 9140, mercury thermometer, SCILOGEX MS 7-H550 Digital Hotplate and computer for data acquisition. The mercury thermometer was immersed in deionized water (MilliQ® was obtained from MILLIPORE water system (USA)—18 MΩ cm) to obtain a continuous temperature reading. Meanwhile, the sensing surface was also immersed in water and collected data when the temperature reached a steady value. The frequency was swapped from 1 Hz to 10000 Hz, to characterize the sensor under different temperatures.

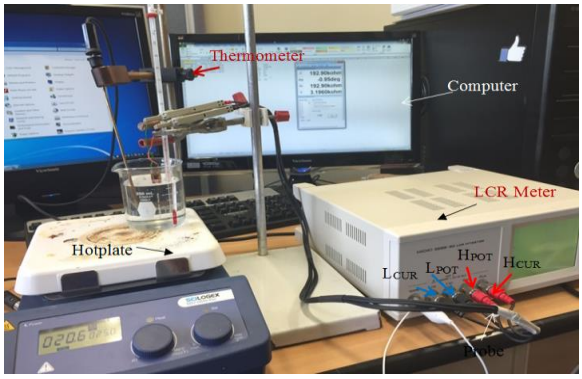

Fig. 3. Experimental arrangement for temperature measurement

The experimental set-up to measure the concentration of nitrate in water is shown in Fig. 4. Ambient temperature and humidity conditions are maintained during experiments. The electronic circuits including the water pump and solenoidal valve are powered from a 12 V battery. The sensor needs an alternating voltage for its excitation. An Arduino Yun [27] has been used to generate a sinusoidal voltage waveform to

provide excitation to the sensor. The sensor measured the temperature

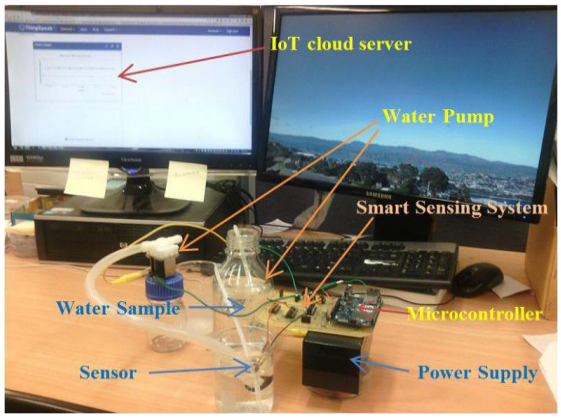

Fig. 4. Experimental arrangement for nitrate-N detection

and the same sensor was used to measure the nitrate concentration. All necessary signal processing was done at the microcontroller. The sensing part of the sensor was dipped in the sample water for measurement. The nitrate ions are polarized towards the plates according to their charge [28]. Two water pumps were used for the experiment; one pump was used to pump the water sample for measurement every 15 minutes and another one was used to discharge the sampled water, after one minute. The Arduino Yun communicates with the cloud server to send the final measured data. All the measurements are taken five times and results averaged .

SENSING SYSTEM

The whole sensing system consists of different circuits with each one performing required operations. The details of the sensor and the sensing system has previously been explained in [21].

A. Equivalent Circuit of Interdigital Sensor

The properties of the sample material are determined from the change of impedance of the interdigital sensor. To determine the impedance of the sensor, a resistance is connected in series with the sensor. The equivalent circuit of the sensor is shown in Fig. 5. The impedance is measured based on the following analysis:

V_{in}: Input voltage applied across the sensor
V_s: Voltage across the series resistance R_s
I_s: Current through the sensor
Z: Total impedance of the sensor

$$I_s = \frac{V_{in}}{Z} \quad (1)$$

$$V_s = I_s \times R_s = \frac{V_{in}}{Z} \times R \quad (2)$$

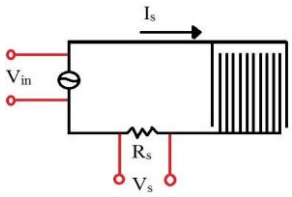

Fig. 5. Equivalent circuit diagram of interdigital sensor

$$Z = \frac{V_{in}}{I_s} = \frac{V_{in}}{V_s} \times R_s \quad (3)$$

B. Working principle of the designed system

Fig. 6 shows the block diagram of the designed system. In this system, the sinusoidal waveform was generated by using PWM (pulse width modulation) output combined with a bandpass filter (Fig. 7), which is based on the concept of the Direct Digital Synthesis (DDS) method. This method was implemented by breaking a waveform into discrete points digitally [29]. Two hundred and fifty-six (8 bits) points were used to produce a sinusoidal waveform that gave a compromise between resolution and frequency. The operating frequency was fixed at 122.5 Hz.

The voltage across R_s is very low. To amplify the voltage as well as to reduce the noise, an amplifier (of gain 10) cum filter circuit in Fig. 8 has been used. The value of the series resistor is 10-kilo ohms, which is significantly small, compared to total impedance. The details of the operation of the circuit shown in Fig. 8 has been explained in [21]. The voltage across the series resistor R_s, is alternating in nature. To rectify the amplified voltage, a precision rectifier, as shown in

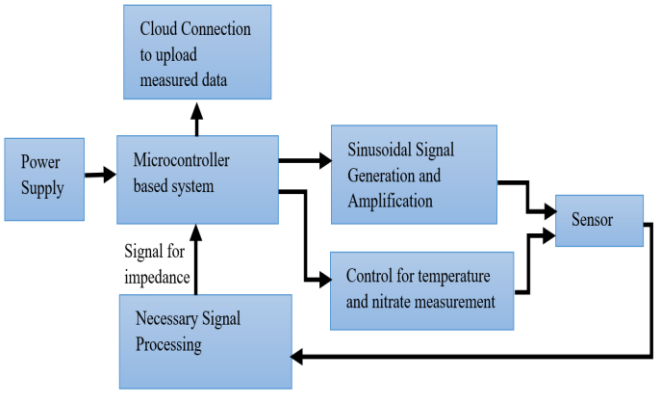

Fig. 6. Block diagram of the designed system

Fig. 9, has been used. The operation has been explained in [21].

In order to calculate the real and imaginary part of the impedance of the sensor, the phase difference between the input voltage, V_{in} and the current, I_s is calculated. The calculation is done inside the microcontroller. The phase difference between V_{in} and I_s is calculated by passing the signals V_{in} and I_s through a zero-crossing detector as shown in Fig. 10. The two square waves are connected to external interrupts of the microcontroller and time difference is calculated internally. The time difference is then converted into the appropriate phase angle. After obtaining the phase difference (ϕ) between V_s and I_s, the components of impedance are calculated as-

$$R = Z \times \cos\emptyset \quad (4)$$

$$X = Z \times \sin\emptyset \quad (5)$$

R and X are the real part and imaginary part of the total impedance of the circuit, as shown in Fig. 6. The actual resistive component of the sensor is given by equ. 6

$$R_{sensor} = \mathrm{R} - \mathrm{Rs} \quad (6)$$

Finally, the resistive component is used to calculate the temperature and eventually, calculating the nitrate concentration.

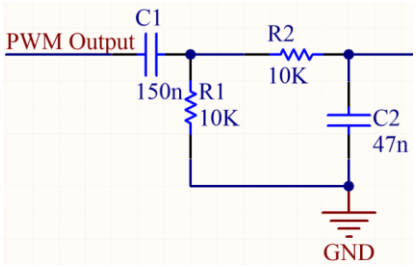

Fig. 7. Band- Pass Filter with PWM output

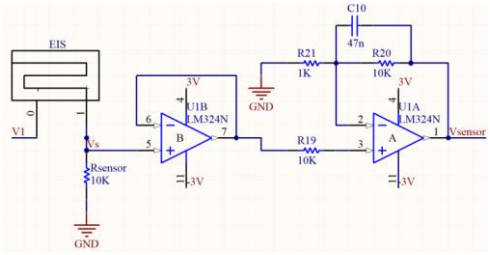

Fig. 8. Amplification circuit after sensor's output

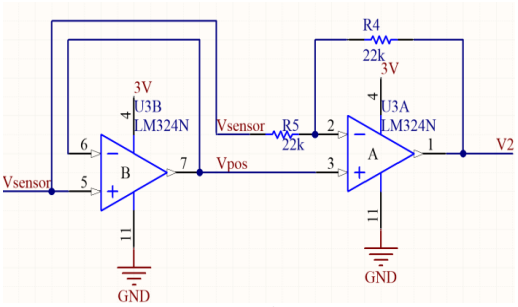

Fig. 9. Rectifier circuit

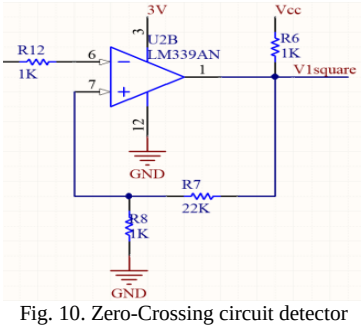

Fig. 10. Zero-Crossing circuit detector

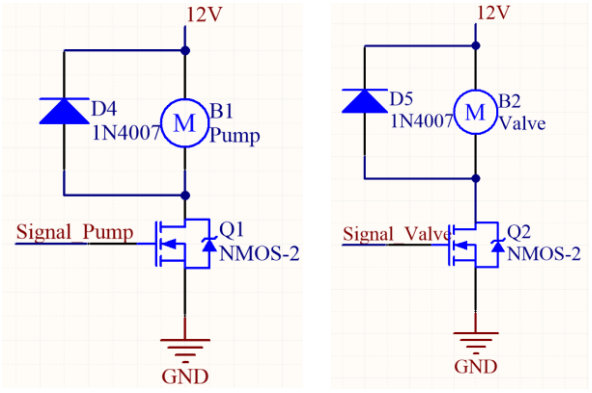

Fig. 11. Control of water flow, pump and valve control

D. IoT-based Smart System

The IoT [30] offers promising solutions to transform the operation and role of existing industrial technologies. IoT is already having an impact in the areas of agriculture, food processing, environmental monitoring, security surveillance and others [31]. The proposed Arduino Yun has integrated WiFi which can provide instant connectivity to the Internet.

C. Control of Pump and Valve

Sample water to be tested for nitrate concentration was pumped in to and out of the sample container, to avoid the sensor being continuously dipped in water. This is achieved using a pump and valve as is shown in Fig. 11. The operation of the circuits has been explained in [21].

WiFi offers high bandwidth, large coverage area, non-line-of-sight transmission, easy expansion, cost-effectiveness, robustness and small distribution of Links [32]. An external antenna (2.4 GHz) is added to increase the transmission signal strength. The collected data is transmitted to Thingspeak [33] which is the open data platform for the IoT. HTTP POST [34] protocol has been used to send data directly to the specified server. Fig. 12 shows the final IoT-based smart sensing system with a smart sensor which has been used to measure nitrate and upload the data on the designated website.

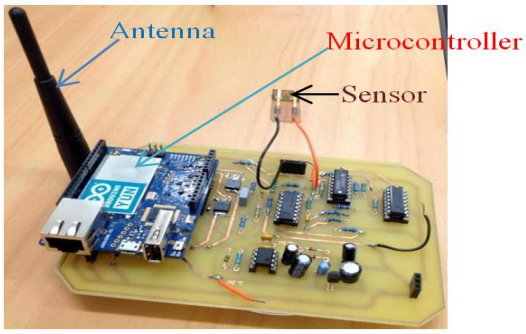

Fig. 12. IoT enabled Smart sensing system

RESULTS AND DISCUSSION

A. Measurement of Temperature

The same sensor was used to measure the temperature of water [35]. The real impedance (R_s) and imaginary impedance (X) were evaluated and plotted in Fig. 13. The X-axis shows the resistance part of impedance in ohms (Ω) and the Y-axis shows the reactance part of the impedance in ohms (Ω). The total impedance is decreased with the increase in temperature. The Nyquist plot (Fig. 13) indicates the impedance at a specific frequency. Fig. 14 shows the relationship between the real part of impedance and the frequency. It is seen from the figure that the resistance is decreased with increasing temperature, and the sensitive range is significant till 400 Hz.

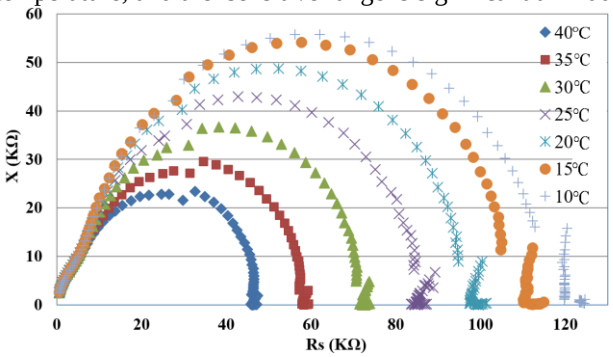

Fig. 13. Nyquist plot of impedance at variable temperatures

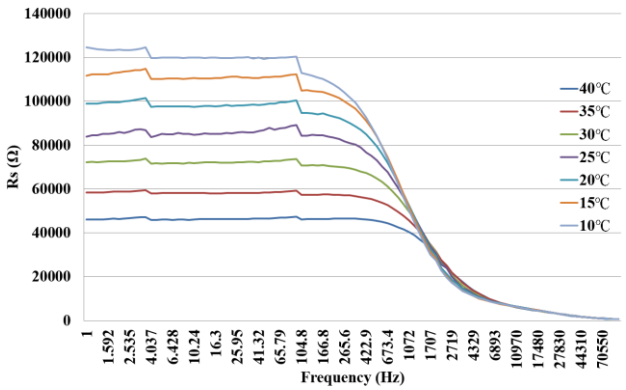

Fig. 14. Real part of impedance vs. frequency under variable temperature

Fig. 15 shows the imaginary part of impedance (X) of deionized water to changing temperature, plotted against frequency. The dielectric properties of the deionized water at different temperatures was measured by using this approach. The experiment was repeated five times to observe impedance behavior and to calculate average results.

Fig. 16 shows the measured resistance as a function of the ambient temperature, which is almost linear. The slope can be calculated by equation 7:

$$Slope = \frac{\Delta R}{\Delta T} = \frac{R_{40} - R_{10}}{T_{40} - T_{10}} \quad (7)$$

where, R_{40}: The resistance value measured at 40˚C, R_{10}: The resistance value measured at 10˚C, T_{40}: The temperature at 40˚C, and T_{10}: The temperatures at 10˚C.

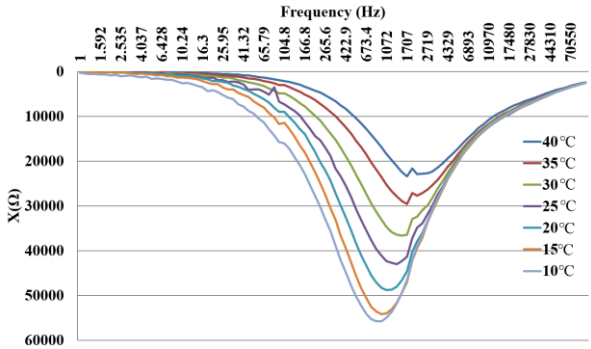

Fig. 15. Imaginary part of impedance as a function of frequency

Therefore, the slope for the resistance part is calculated as- (42392.83 - 118037.76)/ (40-10) = -2521.498. It is to be noted that all the resistance of impedance measurements are taken at the same frequency (122.5 Hz). Therefore, the temperature can be measured by the following equation:

$$T\ (°C) = \frac{R_T - R_{20}}{slope} + T_{20} \quad (8)$$

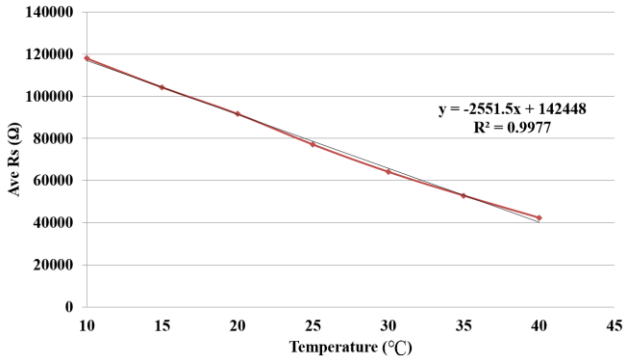

Fig. 16. Resistance as a function of temperature at a frequency of 122.5 Hz

where, R_T is the measured resistance value, R_{20} is the resistance value at 20˚C (which is the reference value), and T_{20} is the reference temperature at 20˚C. Fig. 17 displays the correlation between the actual temperature and the calculated temperature. The calculated temperature is well correlated with the resistance (R^2 = 0.99) part.

B. Nitrate Measurement and Standard Equation Development

The sensing system has been used to detect the concentration of nitrate in water. In the laboratory, samples of different concentrations of ammonium nitrate have been prepared by a serial dilution method with the concentration varying from 0.1 to 0.5 mg/L. The impedance of the sensor is measured using electrical impedance spectroscopy technique and the results are plotted in the Nyquist plot (Fig. 18), when the frequency is restricted to 100 KHz. Tthe impedance of the sensor reduces with increased nitrate concentration. Fig. 19 and Fig. 20 show the real part and imaginary part of impedances as a function of operating frequencies, for different nitrate concentrations.

This article has been accepted for publication in a future issue of this journal, but has not been fully edited. Content may change prior to final publication. Citation information: DOI 10.1109/TIE.2017.2696508, IEEE Transactions on Industrial Electronics

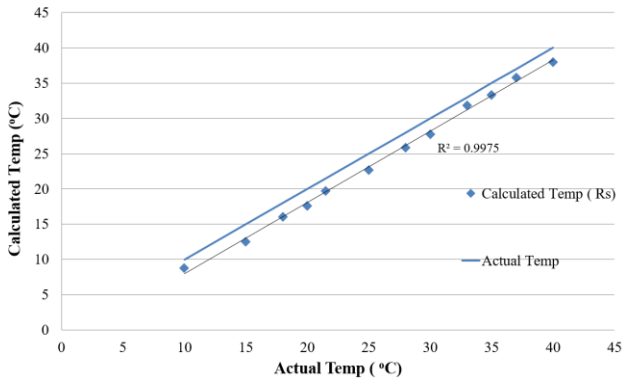

Fig. 17. Comparison between the actual temperature and the measured temperature

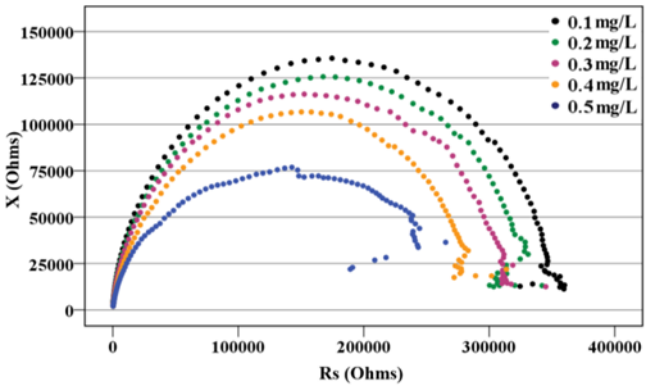

Fig. 18. Nyquist plot for Ammonium Nitrate (NH_4NO_3) at different concentrations

Real part of impedance shows a significant change in their

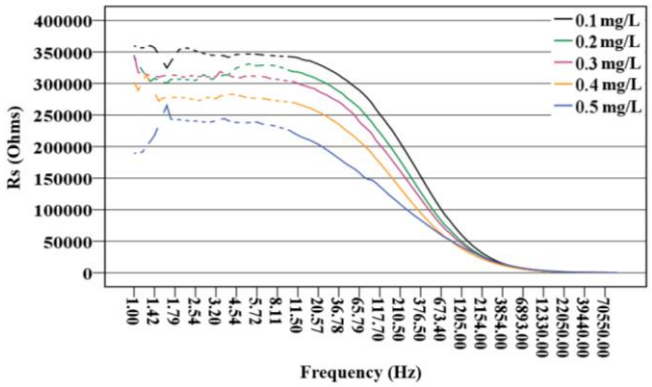

Fig. 19. Real part of impedance as a function of frequency

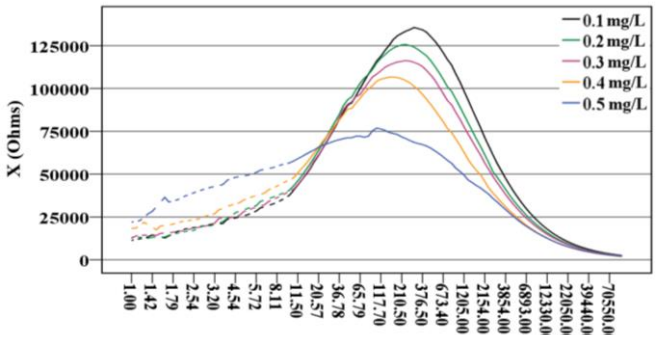

Fig. 20. Imaginary part of Impedance as a function of frequency

value for different concentrations at low frequencies. The imaginary parts do not show a lot of change at low frequencies. Since ionic components play a significant role, the real part of impedance is used to determine the nitrate concentration. The following equation from [21] was derived from the standard curve:

$$C=\frac{R-R_{0.3}}{-115543}+C_{0.3} \quad (9)$$

where R is the real impedance of the sensor using water samples, $R_{0.3}$ is the real part of the impedance at 0.3 mg/L and $C_{0.3}$ represent the concentration of 0.3 mg/L, which is assumed as a reference. Substituting the value of $R_{0.3}$ and $C_{0.3}$ into equation (10), the concentration was calculated by:

$$C=\frac{R-48056.78}{-115543}+0.3 \quad (10)$$

Since the sensor is very sensitive to temperature change, the relationship between the resistance (R) and the temperature (T) can be used as a correction factor for the changing rate of R on changing T. Therefore, using the correction factor, the R_{acutal} is modified by equation 12:

$$R_{actual} = R + \alpha \times (T - T_{20}) \quad (11)$$

where T_{20} is the temperature at 20°C. R is replaced with R_{actual} in equ. 11 to calculate the final computational formula of nitrate-N concentration. Therefore, the standard formula to calculate concentration with a correction factor for the Parylene coated sensor, can be represented by equation 13:

$$C = \frac{R_{actual} - 48056.78}{-115543} + 0.3 \quad (12)$$

This equation has been used to estimate the nitrate concentration in an unknown sample.

C. Stream Water Testing

The next experiment was conducted with stream water samples using the developed sensing system. The water was collected from different streams and was analysed for nitrate using the spectrophotometric method in the laboratory. The developed standard formula in equ. 12 has been used to calculate the concentration using the designed system. Table 1 shows the results from the designed system and the laboratory spectrophotometric method. The spectrophotometric method

Table 1. Comparison of nitrate concentrations measured by the sensor system and the spectrophotometric laboratory method

Lab Number	Description	Spectrophotometric method (mg/L)	Sensor system (mg/L)
S202	Stream entering farm	0.50	0.53
S204	Stream entering wetland	0.49	0.53
S206	Stream paddock 9	0.47	0.51
S207	Stream paddock 10	0.47	0.52
S209	Stream exiting farm	0.50	0.55

was taken as the standard laboratory measurement. The stream water samples not only contain nitrate, but also contain

phosphates, ammonium, and other mineral salts. This explains the differences between these results. Despite this, the maximum error is less than 10% and is low, the reasons being (i) the calibration of sensor was done based on nitrate measurement and (ii) the influence of other ions is not strong with respect to the nitrate ions.

D. Sending Data to IoT-based Cloud Server

In the fourth experiment, the interval time of pump in and pump out of the sample water was 10 minutes and initially deionized water was pumped out and then 0.5 mg/L Ammonium Nitrate (NH_4NO_3) solution was pumped out for the rest of the period. The microcontroller collects the data and sends the final measured data to the Thingspeak server. Fig. **21** shows the real-time data which has been sent from the developed smart sensing system.

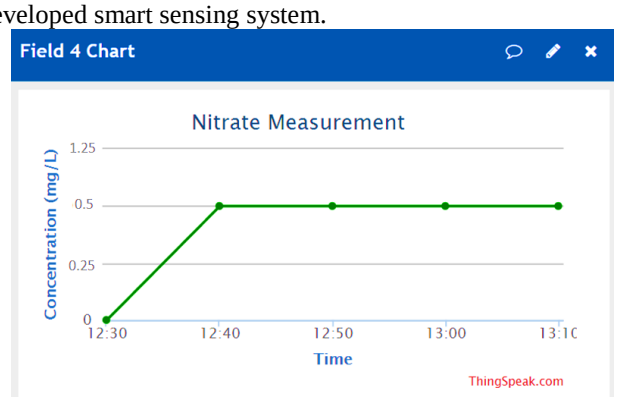

Fig. 21. Final data to the cloud server

E. Comparison of Impedance Measurement by LCR and the Developed System

The fifth experiment was to compare the impedance measurement using the LCR meter and the developed system. Different known concentrations of Ammonium Nitrate (NH_4NO_3) between 0.01 and 0.5 mg/L were measured by the developed system and the LCR meter. Fig. 22 illustrates the test results (NH_4NO_3) from the designed system and LCR meter. When the concentration is increased in the sample, the real part of the impedance decreased accordingly. The corresponding impedance calculation was done inside the microcontroller, and the results of the impedance calculation from the system were very close to the impedance measured by the LCR meter. The designed system showed an excellent linear relation with $R^2 = 0.99$ which is very similar to the LCR impedance measurement.

Fig. 23 shows the comparison of the phase angle between the LCR and the sensor system measurement. During the impedance measurement, the phase angle of the different concentrations was measured. It should be noted that the system's measured phase angles are similar to the LCR measurement and the range of change of phase angle of the

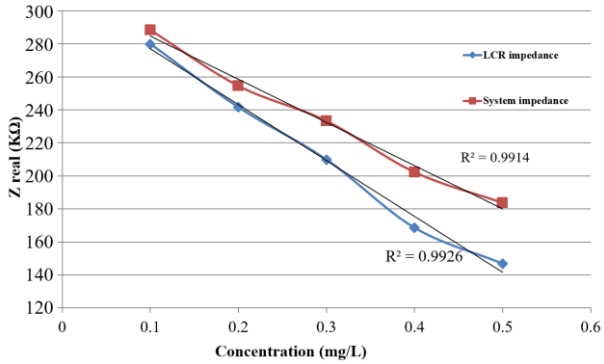

Fig. 22. Comparison of real part of impedance: by LCR and developed system

sensor system, is also similar to that of LCR measurement. The LCR meter has been used to measure the impedance of the Interdigital sensor for different applications. So it is important to compare both results to evaluate the system's performance. The system is capable of running the sensor and recording the data continuously.

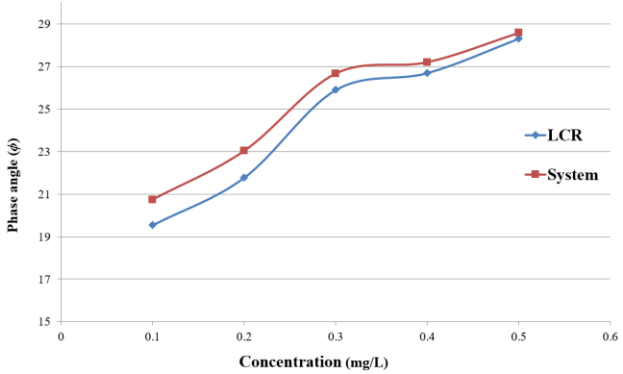

Fig. 23. Comparison of phase angle by LCR and developed system

F. Improvement of Temperature compensation

The last experiment was done to demonstrate the usefulness of the temperature compensation in the developed system. The temperature of the sample water was maintained at 30°C. The concentration of nitrate was measured by the developed sensing system and laboratory spectrophotometric method. Table 2 compares nitrate concentrations measured before and after temperature compensation and calculated using equations 11 and 13,respectively. The error rate was higher (more than 20%) when the temperature change was not compensated in the developed system (Table 3).

Table 2. Comparison of nitrate measurement before and after the temperature compensation.

Sample Number	Sensor System		Spectrophotometric method (mg/L)
	Before Compensation (mg/L)	After Compensation (mg/L)	
1	0.61	0.53	0.50
2	0.59	0.51	0.49
3	0.61	0.50	0.48
4	0.41	0.35	0.33
5	0.43	0.30	0.32

CONCLUSION

Further to our earlier work [21], a temperature compensated interdigital capacitive sensor has been developed in the current study to measure nitrate at low concentrations. A portable, novel sensing system has been developed that could be used on-site as a stand-alone device, as well as IoT-based remote monitoring smart sensor node, to measure nitrate concentration in surface and ground water. Electrochemical Impedance Spectroscopy was employed to detect and display nitrate concentrations, by evaluating the impedance change read by the interdigital transducer immersed in the surface water samples. The test samples were evaluated by commercial equipment (LCR meter) and the designed system. These results were also validated using standard laboratory techniques to assess nitrate concentrations in water samples. The designed system showed a good linear relationship between the measured nitrate concentrations (ranged from 0.01 to 0.5 mg/L) to those measured by the commercial equipment in the collected water samples. However, the current system has the potential to be used to estimate nitrate concentrations in water samples, in real-time. The system can upload the measured nitrate data on a website based on IoT. This system could be used to integrate water quality monitoring sites within farms, or between streams, rivers, and lakes. For the in-situ installation, a robust box containing the whole system would need to be installed at the monitoring site.

ACKNOWLEDGMENT

The authors would like to thank the School of Engineering and Advanced Technology and Institute of Agriculture and Environment, Massey University for providing laboratory facilities for experimentations.

REFERENCES

[1] H. Di and K. Cameron, "How does the application of different nitrification inhibitors affect nitrous oxide emissions and nitrate leaching from cow urine in grazed pastures?," *Soil Use and Management*, vol. 28, pp. 54-61, 2012.

[2] J. Dymond, A.-G. Ausseil, R. Parfitt, A. Herzig, and R. McDowell, "Nitrate and phosphorus leaching in New Zealand: a national perspective," *New Zealand Journal of Agricultural Research*, vol. 56, pp. 49-59, 2013.

[3] L. Kellman and C. Hillaire-Marcel, "Evaluation of nitrogen isotopes as indicators of nitrate contamination sources in an agricultural watershed," *Agriculture, ecosystems & environment*, vol. 95, pp. 87-102, 2003.

[4] P. J. Thorburn, J. S. Biggs, K. L. Weier, and B. A. Keating, "Nitrate in groundwaters of intensive agricultural areas in coastal Northeastern Australia," *Agriculture, ecosystems & environment*, vol. 94, pp. 49-58, 2003.

[5] DairyNZ. (2013, 27/02/2017). *Nutrient management on your dairy farm*. Available: https://www.dairynz.co.nz/media/757901/nutrient_management_on_your_dairy_farm.pdf

[6] C. O. R. WATERS, "Water quality and chemistry in running waters."

[7] A. Ghani, K. Müller, M. Dodd, and A. Mackay, "Dissolved organic matter leaching in some contrasting New Zealand pasture soils," *European Journal of Soil Science*, vol. 61, pp. 525-538, 2010.

[8] W. H. Organization. (2017, 27/02/2017). *Water-related diseases*. Available: http://www.who.int/water_sanitation_health/diseases-risks/diseases/methaemoglob/en/

[9] E. P. Agency. (2017, 27/02/2017). *Ground Water and Drinking Water*. Available: https://www.epa.gov/ground-water-and-drinking-water/table-regulated-drinking-water-contaminants

[10] B. Narayana and K. Sunil, "A spectrophotometric method for the determination of nitrite and nitrate," *Eurasian Journal of Analytical Chemistry*, vol. 4, pp. 204-214, 2009.

[11] K. Horita and M. Satake, "Column preconcentration analysis–spectrophotometric determination of nitrate and nitrite by a diazotization–coupling reaction," *Analyst*, vol. 122, pp. 1569-1574, 1997.

[12] K. M. Miranda, M. G. Espey, and D. A. Wink, "A rapid, simple spectrophotometric method for simultaneous detection of nitrate and nitrite," *Nitric oxide*, vol. 5, pp. 62-71, 2001.

[13] A. Dudwadkar, N. Shenoy, J. Joshi, S. D. Kumar, H. Rao, and A. Reddy, "Application of ion chromatography for the determination of nitrate in process streams of thermal denitration plant," *Separation Science and Technology*, vol. 48, pp. 2425-2430, 2013.

[14] X.-H. Pham, C. A. Li, K. N. Han, B.-C. Huynh-Nguyen, T.-H. Le, E. Ko, *et al.*, "Electrochemical detection of nitrite using urchin-like palladium nanostructures on carbon nanotube thin film electrodes," *Sensors and Actuators B: Chemical*, vol. 193, pp. 815-822, 2014.

[15] X. Wang, Y. Wang, H. Leung, S. C. Mukhopadhyay, M. Tian, and J. Zhou, "Mechanism and experiment of planar electrode sensors in water pollutant measurement," *IEEE Transactions on Instrumentation and Measurement*, vol. 64, pp. 516-523, 2015.

[16] B. Schazmann and D. Diamond, "Improved nitrate sensing using ion selective electrodes based on urea-calixarene ionophores," *New Journal of Chemistry*, vol. 31, pp. 587-592, 2007.

[17] B. A. Pellerin, B. A. Bergamaschi, B. D. Downing, J. F. Saraceno, J. D. Garrett, and L. D. Olsen, "Optical techniques for the determination of nitrate in environmental waters: Guidelines for instrument selection, operation, deployment, maintenance, quality assurance, and data reporting," US Geological Survey 2328-7055, 2013.

[18] A. A. Ensafi and M. Amini, "Highly selective optical nitrite sensor for food analysis based on Lauth's violet–triacetyl cellulose membrane film," *Food Chemistry*, vol. 132, pp. 1600-1606, 2012.

[19] M. A. M. Yunus, S. Ibrahim, W. A. H. Altowayti, G. P. San, and S. C. Mukhopadhyay, "Selective membrane for detecting nitrate based on planar electromagnetic sensors array," in *Control Conference (ASCC), 2015 10th Asian*, 2015, pp. 1-6.

[20] G. Pandey, R. Kumar, and R. J. Weber, "Real time detection of soil moisture and nitrates using on-board in-situ impedance spectroscopy," in *2013 IEEE International Conference on Systems, Man, and Cybernetics*, 2013, pp. 1081-1086.

[21] M. E. Alahi, L. Xie, A. I. Zia, S. Mukhopadhyay, and L. Burkitt, "Practical nitrate sensor based on electrochemical impedance measurement," in *Instrumentation and Measurement Technology Conference Proceedings (I2MTC), 2016 IEEE International*, 2016, pp. 1-6.

[22] L. Xie, A. I. Zia, S. Mukhopadhyay, and L. Burkitt, "Electrochemical impedimetric sensing of nitrate contamination in water," in *2015 9th International Conference on Sensing Technology (ICST)*, 2015, pp. 257-262.

[23] A. V. Mamishev, K. Sundara-Rajan, F. Yang, Y. Du, and M. Zahn, "Interdigital sensors and transducers," *Proceedings of the IEEE*, vol. 92, pp. 808-845, 2004.

[24] M. S. A. Rahman, S. C. Mukhopadhyay, P.-L. Yu, J. Goicoechea, I. R. Matias, C. P. Gooneratne, *et al.*, "Detection of bacterial endotoxin in food: New planar interdigital sensors based approach," *Journal of Food Engineering*, vol. 114, pp. 346-360, 2013.

[25] A. I. Zia, A. M. Syaifudin, S. Mukhopadhyay, P. Yu, I. Al-Bahadly, C. P. Gooneratne, *et al.*, "Electrochemical impedance spectroscopy based MEMS sensors for phthalates detection in water and juices," *Journal of Physics: Conference Series*, vol. 439, p. 012026, 2013.

[26] R. L. Miller, W. L. Bradford, and N. E. Peters, *Specific conductance: theoretical considerations and application to analytical quality control*: US Government Printing Office, 1988.

[27] A. B. Yun, "URL: https://www. arduino. cc/en/Main," ed: ArduinoBoardYun.
[28] A. M. Syaifudin, M. Yunus, S. Mukhopadhyay, and K. Jayasundera, "A novel planar interdigital sensor for environmental monitoring," in *Sensors, 2009 IEEE*, 2009, pp. 105-110.
[29] A. Prodic, D. Maksimovic, and R. W. Erickson, "Design and implementation of a digital PWM controller for a high-frequency switching DC-DC power converter," in *Industrial Electronics Society, 2001. IECON'01. The 27th Annual Conference of the IEEE*, 2001, pp. 893-898.
[30] L. Liao, W. Jin, and R. Pavel, "Enhanced restricted boltzmann machine with prognosability regularization for prognostics and health assessment," *IEEE Transactions on Industrial Electronics*, vol. 63, pp. 7076-7083, 2016.
[31] L. Da Xu, W. He, and S. Li, "Internet of things in industries: A survey," *IEEE Transactions on industrial informatics*, vol. 10, pp. 2233-2243, 2014.
[32] L. Li, H. Xiaoguang, C. Ke, and H. Ketai, "The applications of wifi-based wireless sensor network in internet of things and smart grid," in *Industrial Electronics and Applications (ICIEA), 2011 6th IEEE Conference on*, 2011, pp. 789-793.
[33] (2016). *Thingspeak: The open data platform for the Internet of Things*. Available: https://thingspeak.com/
[34] T. Berners-Lee, R. Fielding, and H. Frystyk, "Hypertext transfer protocol--HTTP/1.0," 2070-1721, 1996.
[35] M. E. E. Alahi, X. Li, S. Mukhopadhyay, and L. Burkitt, "Application of Practical Nitrate Sensor Based on Electrochemical Impedance Spectroscopy," in *Sensors for Everyday Life: Environmental and Food Engineering*, S. C. Mukhopadhyay, O. A. Postolache, K. P. Jayasundera, and A. K. Swain, Eds., ed Cham: Springer International Publishing, 2017, pp. 109-136.

Md. Eshrat E Alahi was born in Dhaka, Bangladesh. He received his B.Sc in Electrical Engineering in 2007 from Military Institute of Science and Technology (MIST), Bangladesh. He also received his M.Sc. in Information and Automation Engineering from University of Bremen, Germany in 2013. He is a student member of IEEE since 2015.Currently he is pursuing his PhD in Electronic Engineering in Macquarie University, Sydney, Australia and his research interests are smart sensing system, Internet of things and embedded system.

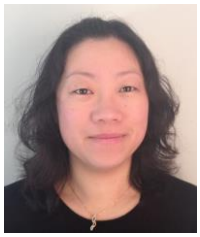

Xie Lie received the B.E. and M.E. degree in Electronic engineering from the School of Engineering and Advanced Technology, Massey University, New Zealand, in 2014, and 2015 respectively. She has interests on embedded electronics and system design.

Subhas Mukhopadhyay holds a B.E.E. (gold medallist), M.E.E., Ph.D. (India) and Doctor of Engineering (Japan). He has over 26 years of teaching, industrial and research experience.

Currently he is working as a Professor of Mechanical/Electronics Engineering, Macquarie University, Australia and is the Discipline Leader of the Mechatronics Engineering Degree Programme. Before joining Macquarie he worked as Professor of Sensing Technology, Massey University, New Zealand. His fields of interest include Smart Sensors and sensing technology, instrumentation techniques, wireless sensors and network (WSN), Internet of Things (IoT), numerical field calculation, electromagnetics etc. He has supervised over 40 postgraduate students and over 100 Honours students. He has examined over 50 postgraduate theses.

He has published over 400 papers in different international journals and conference proceedings, written six books and thirty-six book chapters and edited fifteen conference proceedings. He has also edited twenty-five books with Springer-Verlag and seventeen journal special issues. He has organized over 20 international conferences as either General Chairs/co-chairs or Technical Programme Chair. He has delivered 292 presentations including keynote, invited, tutorial and special lectures.

He is a Fellow of IEEE (USA), a Fellow of IET (UK), a Fellow of IETE (India), a Topical Editor of IEEE Sensors journal, and an associate editor of IEEE Transactions on Instrumentation and Measurements. He is a Distinguished Lecturer of the IEEE Sensors Council from 2017 to 2019. He chairs the IEEE IMS Technical Committee 18 on Environmental Measurements.

Lucy Burkitt was born in Australia. She received a B. of Agricultural Science in 1998 from LaTrobe University, Australia and a PhD. (Soil Science) from LaTrobe University, Australia in 2003.She was a Researcher at the University of Tasmania for 10 years, specializing in soil nutrient management and nutrient loss. She is currently a Senior Researcher at Massey University specializing in reducing the impacts of agriculture on water quality and high frequency water quality monitoring. Dr Burkitt was editor of the joint Australian and New Zealand Society of Soil Science Conference Proceedings in 2012 and a member of the organizing committee for this conference in 2012 and 2016.